AL_2O_3 - DISPERSION STRENGTHENED NANOCRYSTALLINE COPPER

K. Ďurišinová, J. Ďurišin, M. Orolínová

Abstract

This paper is centred on the microstructure evolution in Cu-Al_2O_3 composite after processing of the nanocrystalline powder into a macroscopic compact, as well as thermal loading of the solid at elevated temperatures. The effect of dispersed oxide phase on the preservation of the initial nanostructure with mean crystallite size of 11 nm is analysed. The study shows that uniformly distributed γ–Al_2O_3 nano-particles effectively strengthen grain boundaries during consolidation processes. The as-extruded composite has a stable microstructure nearly up to 800°C. The result of the homogeneous fine-grained microstructure is good hardness and tensile strengths but too small of a ductility which is characteristic for nanomaterials.

Keywords: powder metallurgy, nanocrystalline copper, dispersoid, microstructure, thermal stability, tensile properties

INTRODUCTION

Dispersion strengthened Cu–Al_2O_3 composite materials are extensively used as materials for products such as electrode materials for lead wires and spot welding, relay blades and contact supports that require high strength at a high temperature, wear-resistance for electrical discharge as well as electrical properties [1]. The main requirement for structure of dispersion strengthened materials is a homogeneous distribution of very fine oxide particles (dispersoids) in the copper matrix. In nanocrystalline materials, the main role of the dispersoids is to limit grain growth at elevated temperatures and to attain a very small grain size, resulting in high strength due to the fine-grain strengthening mechanism [2].

Our work deals with microstructural evolution in the Cu–Al_2O_3 composite, wherein the secondary phase represents 3 vol.%. The study analyses the influence of dispersoids on the stabilization of the powder nanostructure during consolidation and structural stability of the solid at elevated temperatures.

MATERIAL PREPARATION AND METHODS

The Cu–3 vol.% of γ–Al_2O_3 mixture was prepared by the combination of mechanical milling with phase transformations of the precursors. The preparation is described in detail in our works [3,4]. The method resulted in the formation of the nanocrystalline powder with an average Cu crystallite size of 11.1 nm (see Tab.1). Obtained by in situ γ–alumina particles are ultrafine – about 20 nm in diameter. The morphology and particle size of the mixture is documented in Fig.1. The densification consisted of pressing in protective atmosphere under pressure of 150 MPa, sintering in H_2 at 850ºC for 1h, forging and subsequent extrusion at 950ºC into bar form.

Katarína Ďurišinová, Juraj Ďurišin, Mária Orolínová, Institute of Materials Research, Slovak Academy of Sciences, Watsonova 47, 043 53 Košice, Slovak Republic

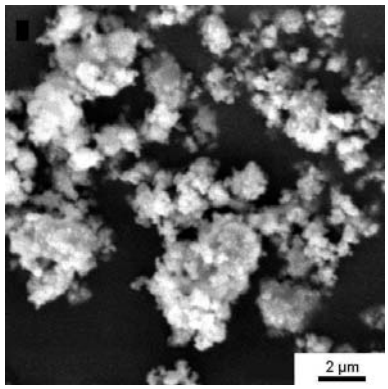

Fig.1. SEM picture of the as-prepared Cu–Al_2O_3 powder.

The powder and the samples prepared from the extruded bars in the longitudinal and cross directions, with respect to the direction of extrusion, were analyzed. The evolution of the nanostructure was followed by optical microscopy, scanning electron microscopy (SEM) and transmission electron microscopy (TEM), as well as X–ray diffraction (XRD) using Cu Kα radiation over a 2θ range of 42–77°. The crystallite size was determined by the Scherrer formula [5]. Structural stability after 1h annealing in H_2 at 200 to 800°C was tested indirectly, by means of the Brinell hardness. The tensile tests of specimens (ϕ 3 and 15 mm long) were carried out at room temperature by universal test machine Tiratest 2 300 at a crosshead speed of 2 mm/min. The electrical conductivity was estimated using measurements on the RLC-bridge.

Tab.1. The changes of the relative intensity $I_{rel.}$ of (111), (200) and (220) peaks and the copper crystallite sizes D after compaction of the Cu–Al_2O_3 powder.

		(111)		(200)		(220)	
		$I_{rel.}$ [%]	D [nm]	$I_{rel.}$ [%]	D [nm]	$I_{rel.}$ [%]	D [nm]
As-prepared powder		100	15.9	45	9.0	25	9.4
As-extruded composite	longitudinal direction	36	24.3	100	31.2	59	26.8
	cross direction	90	27.5	100	21.8	2	-
Cu after JCPDS*		100		46		20	

*Joint Committee on Powder Diffraction Standards

RESULTS

Comparison of the changes in the average crystallite size of the powder and the as-extruded material reveals that compacting resulted in some coarsening of the structure, but the newly formed microstructure remained in the nanometric range, Tab.1. The rough microstructure observed by optical microscopy is homogeneous with a high fraction of the interfaces. Some micropores are present as well. A typical TEM microstructure is documented in Fig.2. From the TEM analysis it results that the Cu–3 vol.% of γ–Al_2O_3 alloy consists of a fine grain structure arranged into parallel rows to the applied stress during extrusion and approximately equiaxed grains in the transverse cross section, strengthened by the nanometric ceramic particles distributed fairly uniformly within the copper matrix. Complex dislocation structures characteristic of a heavily deformed material are evident in

many areas. The fine polygon grains are fragmented into a cell substructure. The copper crystallite/cell size *D* determined by the XRD profile analysis is in the 24.3–31.2 nm range, Tab.1. The γ–Al_2O_3 dispersoids with the size of 20 to 50 nm are located mostly at the grain/cell boundaries, and dislocations commonly interact with them. Coarser alumina clusters are observed as well. The grain structure is not completely developed, but rather consists of diffuse, poorly defined boundaries. The boundaries are kinked or curved as well as wider where pinning particles are present, as is shown in Fig.2. The alumina dispersoids postpone the recovery because of blocking the cross slip and climbing of dislocations to a certain extent, and play a key role in stabilizing both the grain structure and dislocation substructure introduced during powder preparation and subsequent hot extrusion. For copper, the typical presence of the deformation twins was not recorded. This indicates that the prevailing mechanism of the plastic deformation during densification is the slip movement of dislocations. The movement is partially restrained by the secondary phase particles that concurrently prevent the formation of the twins as a result of heating

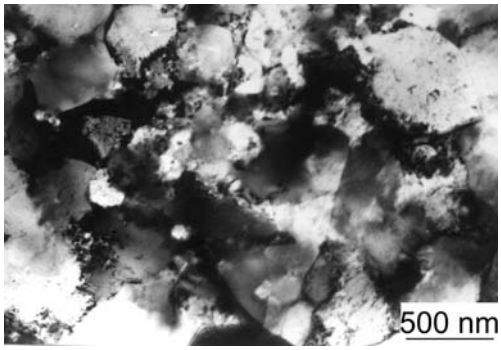

Fig.2. TEM image of the as-extruded Cu–Al_2O_3 microstructure (cross direction).

The X-ray diffraction patterns of the powder entering the consolidation process and the as-extruded material in Fig.3 point out that the changes of the (111), (200) and (220) peak intensities occurred by the compaction of the mixture. In Table 1, the values of the relative intensities of those diffraction lines are recorded. The preferential grain orientation testifies as to the deformation texture formation.

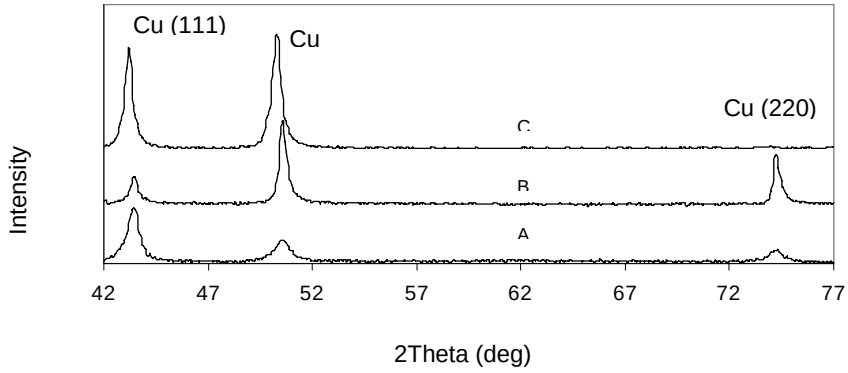

Fig.3. X-ray diffraction patterns of the Cu-Al_2O_3 material: as-prepared powder (A), as-extruded material – longitudinal (B) and cross (C) direction.

Figure 4 illustrates the Brinell hardness measured at room temperature and after different heat treatment up to 800°C for 1 h in H_2. The figure documents markedly enhanced hardness of the composite compared to pure coarse-grained Cu resulting from ultrafine microstructure, as exemplified by the commonly known Hall-Petch relationship between the yield strength/hardness and grain size. The Cu – Al_2O_3 material exhibit a slow hardness reduction above 700°C, suggesting thermal structural stability over the probed temperature range.

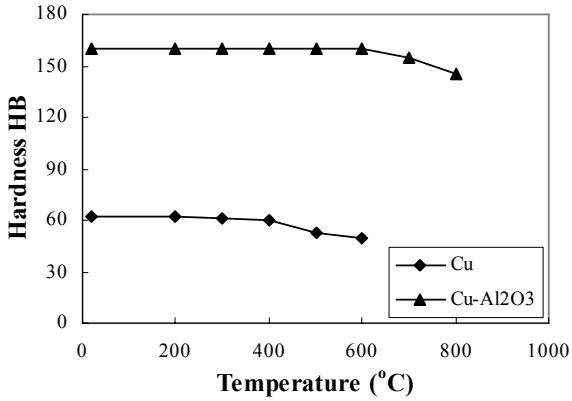

Fig.4. Brinell hardness vs. annealing temperature for ultrafine Cu–Al_2O_3 and coarse-rained Cu.

Table 2 gives an overview of the room temperature results of the tensile tests, hardness and electrical conductivity of the Cu-Al_2O_3 in contrast to the pure, coarse-grained Cu compacted by the same method as the composite samples. The Cu–Al_2O_3 alloy shows appreciable strength properties due to the strengthened matrix grains ranging in nanometric scale (see Table 1). On the contrary, the elongation of Cu–Al_2O_3 is low, only 2%, what is the usual value for nanomaterials with a homogeneous structure. The room temperature fracture surface mainly consists of dimples and also small regions of intense shear where all details are smeared out, as shown in Fig.5. The dimples are on the order about 1 μm, thus considerably larger than the grain size. A coarser second phase particles are often situated at the bottom of the dimples. It is reasonable to assume that the dimple size is determined by the inclusions, as well as the spacing of other initiation sites as are micro-pores, voids, cracks of a critical dimension that interact and produce the final dimple size.

Tab.2. Comparison of the ultrafine copper composite and coarse-grained pure copper properties.

	Yield strength [MPa]	Ultimate tensile strength [MPa]	Ductility [%]	Brinell hardness HB	Electrical conductivity [% IACS]
Cu-Al2O3	397	436	2	160	62
Cu	100	135	22	62	100

The electrical conductivity of the composite material is reduced; however, the value of 62% IACS is still satisfactory for electrotechnical applications, Tab.2.

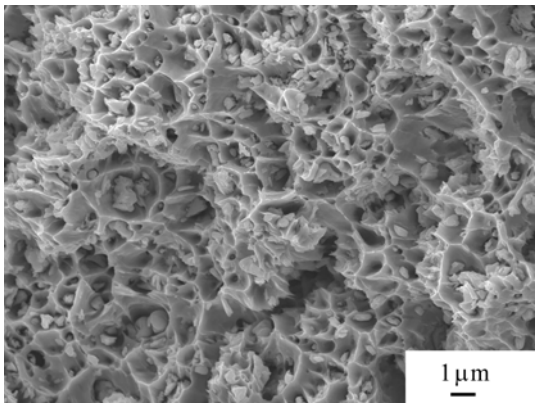

Fig.5. SEM micrograph of the Cu –Al_2O_3 fracture surface with dimpled structure.

CONCLUSION

A nanocrystalline Cu – 3 vol.% of γ-Al_2O_3 mixture with the mean copper crystallite size of 11.1 nm was prepared by the combination of mechanical milling with the phase precursor transformations.

Fine and uniformly distributed alumina nanoparticles effectively limit grain growth and maintain its nanometric size during consolidation. The composite solid has a stable microstructure nearly up to 800°C. The result of the homogeneous fine-grained microstructure is good hardness and tensile strengths, but too small of a ductility, which is characteristic for nanomaterials.

Acknowledgement

The above-presented research was funded under the Slovak Agency for Science VEGA within project No. 2/4172/26.

REFERENCES

[1] Lee, DW., Ha, GH., Kim, BK.: Scripta Mater., vol. 44, 2001, p. 2137
[2] Takida, T., Mabuchi, M., Nakamura, M., Igarashi, T., Doi, Y., Nagae, T.: Metall. Mater.Trans. A, vol. 31, 2000, p. 715
[3] Orolínová, M., Ďurišin, J., Medvecký, Ľ., Ďurišinová, K.: Journal of Materials Science Letters, vol. 20, 2001, p. 119
[4] Ďurišin, J., Ďurišinová, K., Orolínová, M., Saksl, K.: Int. J. Materials and Product Technology, vol. 23, 2005, Nos.1/2, p. 42
[5] Klug, HP., Alexander, LE.: X-Ray Diffraction Procedures. New York : J. Wiley & Sons, Inc., 1974.